This is an Accepted Manuscript of an article published by Taylor & Francis Group in QIRT Journal on 04/05/2017, available online: https://doi.org/10.1080/17686733.2017.1320885

Active dynamic thermography method for TRAM flap blood perfusion mapping in breast reconstruction

M. Moderhak[a], Sz. Kołacz[b], J. Jankau[b] and T. Juchniewicz[a]

[a]Gdansk University of Technology, Gdansk, Poland; [b]Gdansk University of Medicine, Gdansk, Poland

ABSTRACT

This paper presents the new method of the transverse rectus abdominis musculocutaneous flap blood perfusion mapping based on the active dynamic thermography. The method is aimed at aiding a surgeon during breast reconstruction procedure. A pair of dT_{norm} and t_{90_10} parameters were used as parametric image descriptors of the flap blood perfusion. The method was tested on 38 patients that were subjected to breast reconstruction procedure. This showed that, comparing to the static thermography, this is potentially an objective and effective method of skin flap perfusion assessment that can be performed in the operating room.

KEYWORDS

TRAM flap; tissue reconstruction; parametric imaging; Active dynamic thermography

1. Introduction

One of the problems in plastic surgery is tissue reconstruction in patients that underwent cancerous breast resection. The most popular method of such reconstruction is based on unipedicled skin flap transplant to the target area. Among different reconstruction techniques the unipedicled transverse rectus abdominis musculocutaneous (TRAM) flap breast reconstruction is one of the most important ones. The flap utilises blood flow through the deep superior epigastric pedicle within the rectus abdominis muscle [1]. Three different techniques of unipedicled flap are used in this type of reconstruction: (i) IPSI where skin flap is taken with the rectus abdominis muscle that is located at the same side as the reconstructed breast, (ii) CONTRA where the flap is extracted within the muscle diagonally and (iii) TRAM supercharged where the deep superior epigastric pedicle is microsurgical connected with internal thoracic artery [1]. Such coupling (iii) provides better blood perfusion in the reconstructed area and reduces the risk of flap necrosis.

Currently the most popular methods of skin flap evaluation are based on subjective evaluation such as: tissue colour, respecting flap perfusion zones guidelines shown in Figure 1. In the abdominal skin flap 4 zones of different perfusion can distinguished: zone IV has poor blood perfusion and it is usually not considered for reconstruction. Blood perfusion in zones II and III strongly depends on each patient's anatomy. Zone I is considered to be the most reliable for reconstruction [2].

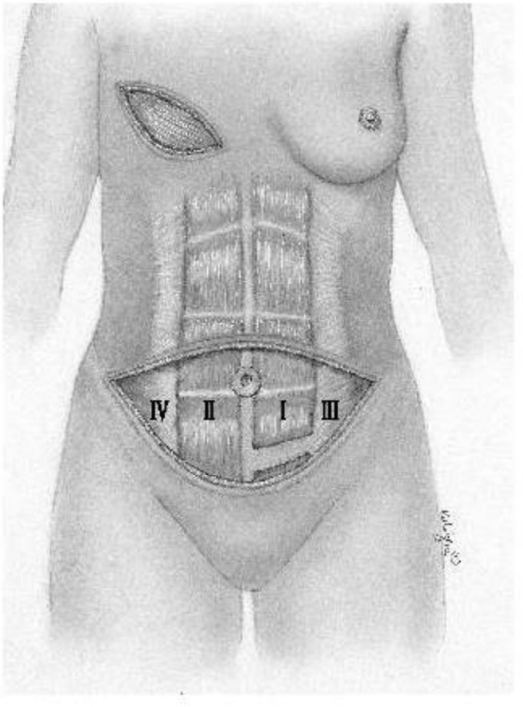

Figure 1. Perfusion zones of the TRAM skin flap; Zone I is the most reliable and zone IV is least suited for reconstruction.

The ideal method for flap blood perfusion imaging should be: patient and flap safe, non-invasive, repeatable, fast as well as yielding low purchase and exploitation costs [3]. Among available methods such as: angiography, angio-CT, on indocyanine green dye [4,5] and MRI, laser Doppler imaging (LDI) and thermography. Thermography is the closest to fulfilling all mentioned requirements. Its functional imaging possibilities enable flap thermal activity monitoring which is the consequence of body blood perfusion and metabolism [6–12]. Thermography is also relatively cheap and accessible compared to other techniques like LDI.

2. ADT imaging, image descriptors

Flap parametric imaging was performed based on the idea of dT_{norm} (formula 1), and t_{90_10} (formula 2, Figure 2) image descriptors that were also applied in the evaluation of cardio-surgery wound healing [13,14] as well as breast cancer detection.

$$dT_{norm} = \frac{dT_{return}}{dT_{excit}} \tag{1}$$

$$t_{90\_10} = t_{10}(T = 0.1 \cdot dT_{return}) - t_{90}(T = 0.9 \cdot dT_{return}) \tag{2}$$

In the case of heating the formula (2) is transformed into (3):

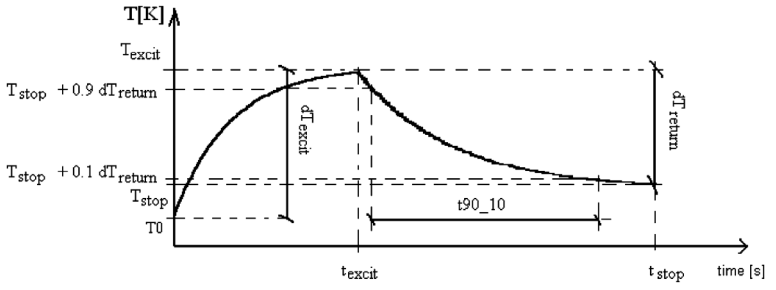

Figure 2. The idea of thermal parametric imaging presented in this paper based on heating excitation.

$$t_{90\_10} = t_{90}(T = 0.9 \cdot \mathrm{d}T_{return}) - t_{10}(T = 0.1 \cdot \mathrm{d}T_{return}) \tag{3}$$

for t_{excit} = 60 s and t_{stop} = 240 s the:

$$t_{90\_10n} = \frac{t_{90\_10}}{180\ \mathrm{s}} \tag{4}$$

where: $T0$ – the initial temperature value of the object, T_{stop} – the termination temperature value of the experiment, T_{excit} – tissue temperature value the moment thermal excitation (heating) is switched off, t_{excit} – the duration of the thermal excitation phase, t_{stop} – time moment of the end of the experiment, $\mathrm{d}T_{excit}$ – total change of the temperature value of the object while heating, $\mathrm{d}T_{return}$ – total drop of the temperature value after switching off the excitation, t_{90_10} – a difference of time, after which the object temperature drops to 10% of $\mathrm{d}T_{return}$ value and time it reached 90% of this value.

The magnitudal parameter $\mathrm{d}T_{norm}$ describes the rate of temperature return relative to the temperature rise caused by tissue heating. If $\mathrm{d}T_{norm}$ value equals 1 this means that the temperature value reached the initial state value within the 180 s, this usually takes place due to tissue high thermal activity (high blood perfusion, metabolic rate, etc.). On the other hand if $\mathrm{d}T_{norm}$ value equals 0 this means that there was no temperature change in the return phase, such situation takes place if there is no thermal activity (low blood perfusion, tissue necrossis, etc…). Additionally, thanks to its normalisation by the $\mathrm{d}T_{excit}$, the $\mathrm{d}T_{norm}$ is independent of the non uniform excitation, which was proved by computer simulation of the active dynamic thermography (ADT) exam in the next sections of this paper.

The temporal t_{90_10} quantifies the speed of the transient process. It is the time period during which the temperature drops from the 90% of its initial value to the 10% of the end temperature. The mathematical model of the ADT thermal transient (heating excitation) is presented in Figure 2. It is a simple alternative to [15–19]. The t_{90_10} values are additionally normalised by the ($t_{stop} - t_{excit}$) factor (formula 4) to unify its value within the 0–1 range. Such operation improves the understanding of the imaging results by the clinics personnel. The case where the value of the normalised t_{90_10} parameter is close to 0 it means that the process of temperature return was very fast, almost instantaneous. This occurs in the areas of high metabolism or high blood perfusion like sought perforators or, it is important to underline that also in the case of necrosis. On the other hand, if the value of the normalised t_{90_10} parameter is close to 1 this means that the process of the temperature value stabilisation was slow. This is the case of the sound tissue. It is important to stress the fact that if the

normalised t_{90_10} parameter value is close to 0 it can mean that the tissue is either very well perfused or dead. This can lead to misinterpretation of the flap perfusion based on single normalised t_{90_10} image. The additional context of high dT_{norm} values, which always indicate high thermal activity complements the information contained in the normalised t_{90_10} image. In practice sought perforators usually appear as the areas of low t_{90_10} values embedded in the areas of high t_{90_10} and dT_{norm} values.

3. Properties of dT_{norm} and t_{90_10n} descriptors in the case of non-uniform thermal excitation

This paragraph mentions the independence of the dT_{norm} and t_{90_10} on parameters of the non-uniform cooling power density. The problem of non-uniform excitation is an important issue of the ADT. Due to the 3D curvature of the flap or the properties of the excitation source, in the practical applications of the ADT, it is hard to provide uniform heating or cooling power density of the whole examined area. The negative influence of this phenomenon on imaging results cause distortions in the amplitude images (the example of such artefacts in the case of dT_{excit} and dT_{return} images are shown in Figure 3). In the case of temporal images like t_{90_10n} (normalised t_{90_10} in formula 4) or time constants such problem theoretically does not exist

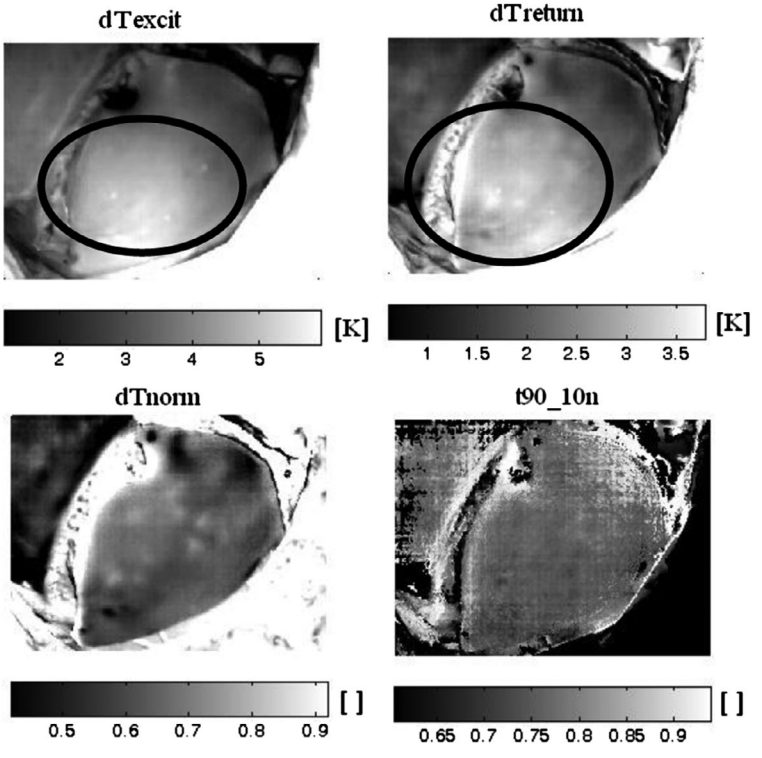

Figure 3. The dT_{excit}, dT_{return}, dT_{norm} and t_{90_10n} parametric images of TRAM flap of heating exam; The dT_{norm} and t_{90_10n}, unlike the dT_{excit} and dT_{return}, reveal no artefacts connected to non-uniform excitation power density of the flap surface; the artefacts are highlighted in black ellipse.

Table 1. The comparison of the mean relative parameter differences (formula 5) of dT_{return}, dT_{norm} and t_{90_10n} for 500 and 1000 W/m^2 excitation power densities.

Parameter type	dPar (%)	Standard deviation (%)
dT_{return}	50.21	0.11
dT_{norm}	0.01	0.02
t_{90-10n}	0.10	0.20

if sufficient signal to noise ratio is provided (e.g. the adequate temperature value rise while heating).

To examine the influence of non-uniform excitation power density on the results of parametric imaging a simulated ADT exam with two cooling power densities of -500 and -1000 W/m^2 was performed. The resulting temperature transient was parameterized using the dT_{norm} and t_{90_10n} values. The results proved that both dT_{norm} and t_{90_10n} descriptors yield similar results independently of the excitation power densities. Such property eliminates the problem of non-uniform excitation of the ADT unit and increases the diagnostic value of the imaging process. Table 1 quantifies dT_{norm} and t_{90_10n} susceptibility to non-uniform excitation power density.

$$\mathrm{dPar} = 100 \cdot \frac{\left|\mathrm{parameter}_{P=500W} - \mathrm{parameter}_{P=1000W}\right|}{\mathrm{parameter}_{P=1000W}}(\%) \tag{5}$$

where: dPar – mean relative parameter difference for 1000 and 500 W/m^2 excitation, parameter$_{P=500W}$ – parameter* value for 500 W/m^2 excitation power densities, parameter$_{P=1000W}$ – parameter* value for 1000 W/m^2 excitation power densities.

*considering dT_{return}, dT_{norm} and t_{90_10n} parameters.

Summing up, the simulations of the ADT exam proved usefulness of the proposed descriptors in blood perfusion imaging of the computer model of the unipedicled skin flap. The dT_{norm} and t_{90_10n} image descriptors provide very good imaging capabilities of the flap thermal activity as well as perforator mapping compared to the static thermography. The results also revealed that the ADT with cooling excitation proved to be more discriminative compared to heating results.

One of the method's big advantages is the dT_{norm} descriptor independence of the non-uniform excitation (shown in Table 1). The influence of the non-uniform excitation on the imaging results is a big disadvantage of the typical magnitude based descriptors like the amplitudes of the exponent components in exponential models of the temperature transients.

4. Practical application

The clinical trials of the TRAM flap blood perfusion imaging method that is presented in this paper was performed in the Clinics of Plastic Surgery at the Medical University of Gdańsk. A series of unipedicled TRAM flap breast reconstructions was performed on 38 patients. This group consisted of 10 IPSI, 11 CONTRA and 17 TRAM supercharged patients [1]. Flap imaging was performed in full anastasia, in thermally controlled (t = 22 °C) operating room. The ADT exam followed the flap separation and elevation. FLIR A320 thermal camera was used for temperature transient recording. The cooling excitation was provided by the TITAN COOL

TC21 portable air conditioner shown in Figure 4 [20]. Heating excitation was performed by the 1000 W matrix of halogen shown in Figure 5, tissue temperature did not exceed 42 °C which is considered safe for the patient. The distance of the lamps from the examined surface was 70 cm. Thermal sequences were recorded by the FLIR Thermacam Researcher v2.9 PRO software.

Each excitation phase lasted 60 s followed by the temperature value decay/rise lasting 180 s. These ADT exam phase duration times were set empirically, based on earlier performed experiments, computer simulations and clinical practice [13,14]. Such acquired data was subjected to post processing procedures involving: image matching based on DPS algorithm, spatial filtration (noise reduction) and finally dT_{norm} and t_{90_10} parameterization and normalisation. To ensure the best quality of thermographic sequence the following guidelines should be provided: minimal patient and ROI movements, object centred in the image as

Figure 4. The ADT imaging unit used in the research

Figure 5. The 1000 W matrix of halogen lamps used in the research as heating excitation.

well as good focus of recorded thermograms. Sequence processing diagram is presented in Figure 6 [13,14,21].

5. Results

The following section presents the representative results of the Transverse Rectus Abdoiminis Flap perfusion imaging. Figure 7 illustrates the specific features of the dT_{norm} and t_{90_10n} parametric images of the flap that are used to localise perforators as well as characterise its thermal activity. The magnitude of the dT_{norm} is proportional to the thermal activity of the flap which is the result of the blood perfusion and metabolism. The areas of high dT_{norm} should only be considered for further reconstruction as they are most likely to be well

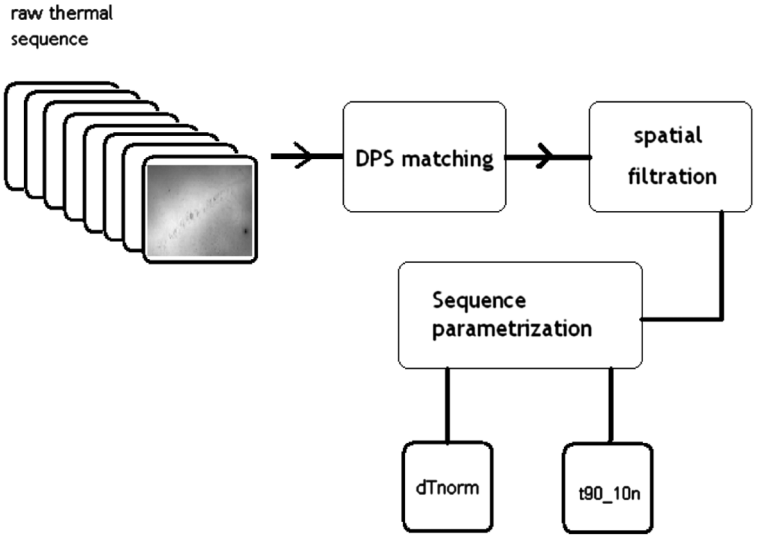

Figure 6. Thermal sequence processing diagram; the input of the raw thermal sequence results in the dT_{norm} and the t_{90_10n} parametric images [10,19,21].

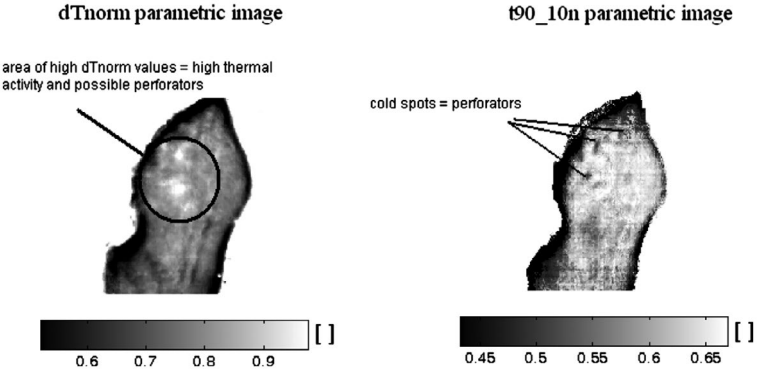

Figure 7. The characteristic features of dT_{norm} and t_{90_10n} parametric images; dT_{norm} describes the thermal activity of the flap as well as the possible perforator locations; t_{90_10n} enables to localise the exact location of perforators.

perfused and contain perforators. The value of the t_{90_10n} image contains the information about the rate of the temperature return to its steady state. Low t_{90_10n} appear when the process of the temperature return is fast, which can suggest high thermal activity of the flap region. On the other hand, it can present itself within the regions that are characterised by poor blood perfusion and metabolism. Such situation usually occurs around the edges of the flap and is confirmed in the dT_{norm} image where low dT_{norm} values suggest poor thermal activity. The most important feature of the t_{90_10n} is the ability to localise the perforators, which are visible as cold spots within the areas of higher t_{90_10n} values.

It is very important to stress the fact that the full qualification of the flap perfusion and localising perforators can be performed only utilising both dT_{norm} and t_{90_10n} parametric images or a single dT_{norm} image which is also useful to indicate the areas of blood perfusion induced thermal activity. The t_{90_10n} image should not be interpreted alone as following only the low t_{90_10n} value criteria can be deceptive.

Table 2 summarises described features and diagnostic properties of the discussed descriptors in flap blood perfusion imaging. The rules of the TRAM flap blood perfusion evaluation were established and verified during the series of the flap tests using the Doppler ultrasound module for the reference (the VENO flow metre device [22]). The Doppler exam was performed before the procedure of breast reconstruction procedure and due to the time consuming manual ultrasound flap scanning only the three largest perforator vessels in zone I were sought. The exemplary result of such USG Doppler flap evaluation for both cooling and heating excitation is presented in Figure 8. The static thermogram of the flap in its steady

Table 2. Summary of the features of the dT_{norm} and t_{90_10n} parameters in TRAM flap blood perfusion assessment.

	dT_{norm} value is high	dT_{norm} value is low
t_{90_10n} value is high	*Well perfused/alive tissue*	*Poor perfusion necrossis*
t_{90_10n} value is low	*Well perfused/'cold spot' in t_{90_10n} image = perforator*	*Poor perfusion necrossis*

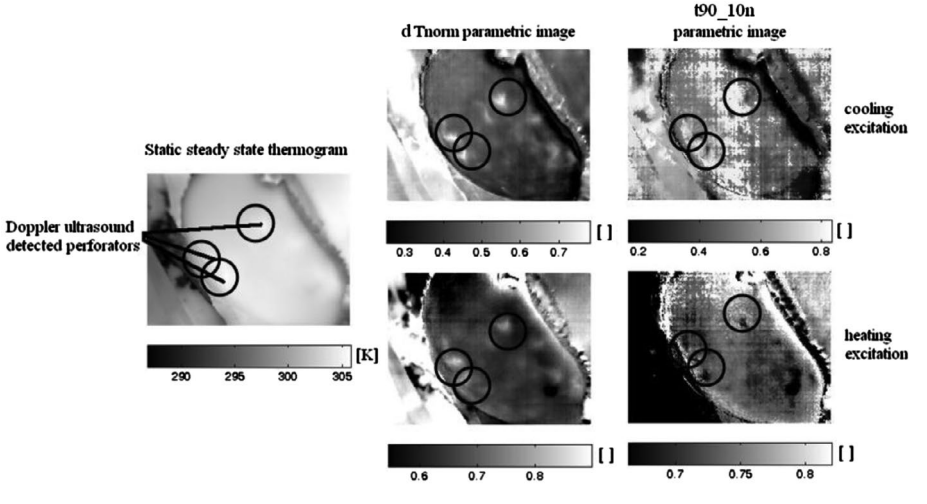

Figure 8. Static thermography imaging, the ADT cooling and heating imaging compared to the USG Doppler; Doppler localised perforators are encircled black in each picture; ADT results match with Doppler results and reveal more potential perforators.

state is also included for comparison. The location of the strongest perforators is encircled in black and corresponds with the location of the three biggest hot spots in dT_{norm} and three biggest cold spots in the t_{90_10n} in both heating and cooling. It is clearly visible that the parametric images reveal more potential perforators. Static thermography, due to its poor contrast, was less sensitive.

The results of the TRAM flap perfusion imaging also show that the guidelines described by Hartramph et al. [2] are not precise. In the case shown in Figure 9 the best perfused area of the flap is located in Zones I and III, with some of the most active perforators located within zone III (zone III is considered as one of the least reliable areas of the TRAM flap). In practice, zone I located directly above the *rectus abdominis* muscle is always directly and strongly perfused in the unipecilted method. However, the quantity of the tissue required for reconstruction is always greater than zone I could provide. In such case Hartrampf recommends acquiring the remaining required tissue from zone II, which in this situation would increase the risk of further partial flap necrosis. Here zone III is much better choice.

6. Static thermography in TRAM flap perfusion monitoring

This section presents the results of a study group of 38 patients undergoing breast reconstruction with a pedicelled skin-muscle TRAM flap, including 10 patients who underwent TRAM IPSI procedure, 10 – TRAM CONTRA and 18 – TRAM supercharged, in which inferior epigastric vessels were additionally anastomosed with internal thoracic vessels. Each patient was examined intraoperatively after the flap was dissected (b2), directly after the procedure was completed when the patient was still in the operating theatre (b3), on Day 1 (b4) and Day 7 (b5) after the procedure. The evaluation included static thermography examination

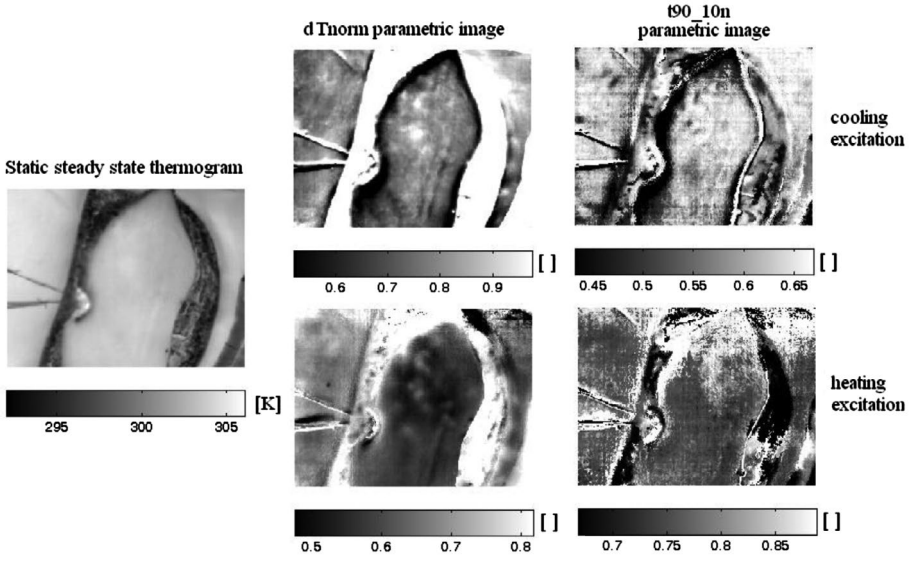

Figure 9. ADT dT_{norm} and normalised t_{90_10n} parametric images characterisation; in dT_{norm} bright spots and in normalised t_{90_10n} dark spots indicate perforator locations in TRAM flap; dT_{norm} shows perfusion induced thermal activity within Zone I and Zone III; t_{90_10n} reveals the location of two very active perforators on the border of the Zone I and III as well as within the Zone III.

and the clinical assessment of blood supply to the flap documented with a photographic examination. All surgical procedures were performed in a thermally stable operating room at 21 °C by the same surgical team and each patient had the opportunity to withdraw from the study at each stage. The study was approved by the Bioethic Committee.

Each operated patient underwent a thermographic examination performed in compliance with the same standards with FLIR A320G camera with spatial resolution of 320×240 pixels and NETD of 0.08 K. The camera was positioned at a distance of 70 cm from the studied flap and perpendicularly to its maximum mound. The first imaging examination was performed immediately after the dissection of the skin-muscle flap and excision of its excesses, second after suturing flap in the recipient region, and the follow-up ones – at 1 and 7 days after the surgery. Each examination consisted of the following steps:

- static thermal imaging with proper thermal adaptation 20 min period
- clinical examination of flap

The collected data were then processed to yield results in a numerical form. In the case of static thermography, we assessed the average temperature Tstat of the flap, expressed in Kelvin degrees.

In order to increase the accuracy of the imaging of skin blood supply disorders in the static tests, each flap was divided into eight zones: 4 central zones (C1, C2, C3, C4) and 4 peripheral zones (B1, B2, B3, B4) shown in Figure 10. The division was always proportional to the size of the examined area.

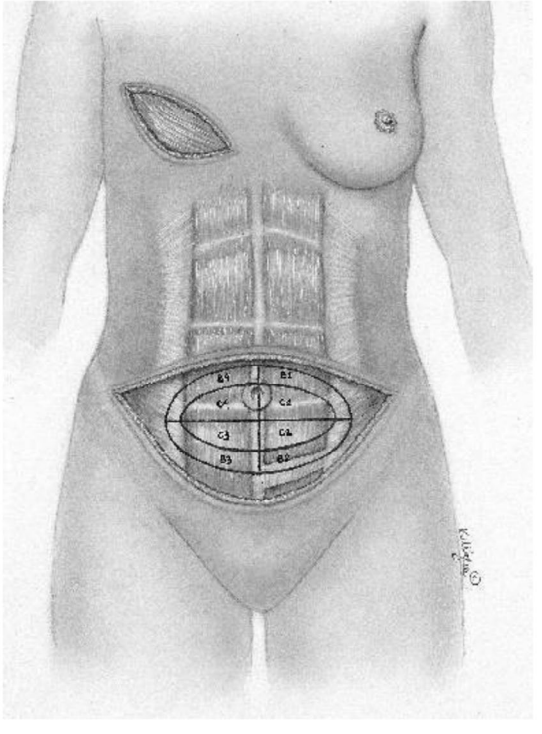

Figure 10. Flap scheme before rotation.

As a result, each piece could be clearly identified despite the change in the spatial arrangement of the flap during reconstructive surgery shown in Figure 11. For each zone both Tstat values were calculated. The obtained data were analysed statistically and compared with the clinical examination results.

Before the initiation of the surgery, the presence of perforators at hot spots of the thermographic examination was confirmed with a Doppler ultrasound probe.

Throughout the period of research photographic documentation was maintained. Throughout the research programme no tissue infection or hematomas developed at the recipient site.

All statistical calculations were performed with the use of a statistical package – StatSoft. Inc. (2011). STATISTICA (data analysis software system) version 10.0 www.statsoft.com and an Excel spreadsheet. Quantitative variables were presented with the use of the arithmetic mean, standard deviation, median, minimum and maximum values (range) and 95% CI (confidence interval), while qualitative variables were presented with the use of frequencies and percentage values. In order to verify whether a quantitative variable came from a normally distributed population the Shapiro-Wilk test was used. The Leven (Brown-Forsythe) test was used to the hypothesis of equal variances.

The significance of differences between the two groups (unpaired variables) was examined with significance difference tests: the Student's *t* (or, in the absence of homogeneity of

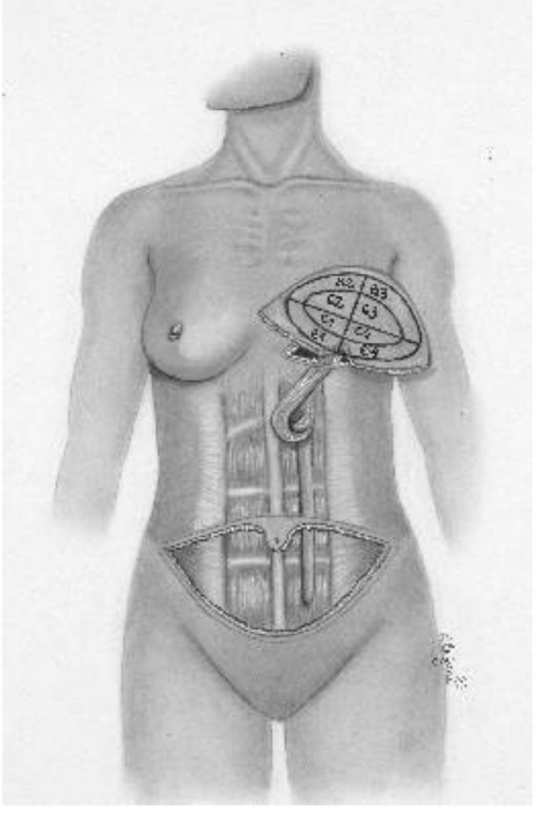

Figure 11. TRAM IPSI after rotation.

variance – Welch test) or Mann–Whitney *U* test (where the conditions of applicability are not met for Student's *t*-test or for variables measured on the ordinal scale). The significance of differences between more than two groups was tested with an *F* test (ANOVA) or Kruskal–Wallis test (where the conditions of applicability are not met for ANOVA). If statistically significant differences were found between groups, *post hoc* tests were applied (Tukey test for F. Dunn – for the Kruskal–Wallis test). In the case of two paired variables Student's t test or Wilcoxon matched pairs test was used (if applicability conditions were not met for the Student t-test or for variables measured on the ordinal scale). The significance of differences between more than two related variables in the model analysis of variance was tested with repeated measurements or Friedman's test (in the case of non-compliance with the applicability of the analysis of variance with repeated measures or for variables measured on an ordinal scale). Chi-square independence tests were used for categorical variables (applying correction by Yates for cell number smaller than 10, verification of Cochran conditions, Fisher's exact test, respectively).

In all the calculations, the level of significance was set at $p = 0.05$.

7. Results

Table 3 presents the results of a comparative analysis of static thermography performed after flap dissection (b2), immediately after flap rotation and suturing and postoperatively (b3): on Day 1 (b4) and 7 (b5) after surgery. Out of 38 patients participating in the study, 9 patients developed marginal necrosis of the skin flap despite intraoperative clinical evaluation of blood supply. No flap developed total necrosis, which would have indicated pedicle tightening or cutting. In the case of TRAM supercharged it would have additionally indicated microsurgical anastomosis obstruction.

Table 3 presents static thermography results. Mean values of necrotic quadrants from all flaps were compared to the mean value of all non-necrotic flaps with respect to examination

Table 3. Comparison of the mean temperature values in K from necrotic quadrants of all flaps in static thermography as per complication incidence in test b-2, b-3, b-4 and b-5.

	Without complications $n = 29$	Complications $n = 9$	p value
b-2			
Mean (SD)	301.64 (1.43)	301.69 (1.42)	
95%CI	[301.47;301.82]	[301.01;302.37]	
Range (min–max)	298.36–304.95	299.93–303.81	
Median	301.50	301.34	0.9341
b-3			
Mean (SD)	301.75 (1.88)	301.79 (2.04)	
95%CI	[301.52;301.97]	[300.80;302.77]	
Range (min–max)	297.68–307.33	299.15–306.44	
Median	301.53	301.83	0.9409
b-4			
Mean (SD)	307.23 (1.51)	305.27 (1.45)	
95%CI	[307.05;307.41]	[304.55;305.99]	
Range (min–max)	302.86–309.90	303.31–308.12	
Median	307.49	305.08	0.0001
b-5			
Mean (SD)	307.20 (1.49)	306.10 (1.51)	
95%CI	[307.03;307.38]	[305.14;307.06]	
Range (min–max)	302.71–311.21	303.41–308.37	
Median	307.32	306.07	0.0165

period. Both in the intraoperative test and in the test performer directly after the flap was sutured onto the recipient site, the standard deviation (SD), the median and the mean value of the temperature did not show statistically significant differences between the flaps with and without complications. After 24 h, however, the difference of all three parameters was significant, which was also confirmed in a thermographic examination on Day 7. Signs of impaired flap perfusion such as skin colour, capillary refill time or flap temperature were visible in a simultaneous clinical evaluation as late as after 24 h and persisted until Day 7, when necrotic tissue was removed. Figures 12 and 13 show images of Patient 6 and static thermograms.

There is no available literature describing the application of static thermography in humans to evaluate pedicled flap perfusion intraoperatively and on subsequent postoperative days, and therefore literature discussion is not possible. Following the analysis of the presented results we think that static thermography does not add significant value to intraoperative evaluation of potential necrosis. It is, however, thoroughly recommended as an imaging examination performed within 24 h after the procedure and on subsequent postoperative days to support and provide adequate documentation of clinical assessment.

8. Discussion

Dynamic thermography has always been seen as a potentially powerful tool for body surface functional imaging [6–9,13–15]. In the case of the unipelicted TRAM flap the close relation between blood perfusion and thermal activity of seems obvious.

The presented method was tested on 38 patients who underwent the breast reconstruction process. Three operating methods were tested: ipsi, contra and TRAM supercharged [1]. Each patient was subject to seven thermal exams: before the procedure, after flap elevation, after flap relocation, 24 h, 7, 30 and 90 days after the reconstruction procedure. Each exam was performed by the statcic thermography, ADT with heating excitation, ADT with cooling excitation as well as the flap manual Doppler ustrasound before the procedure.

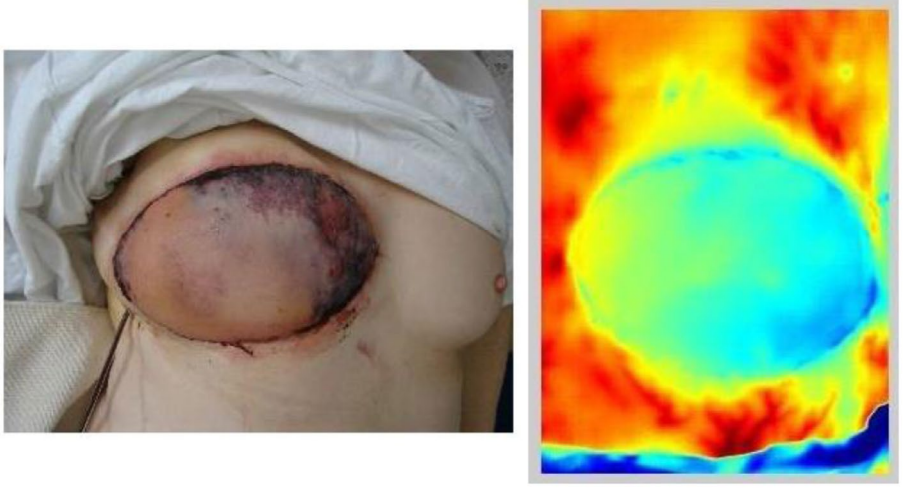

Figure 12. Partial TRAM flap necrosis. Day 7 after surgical procedure.

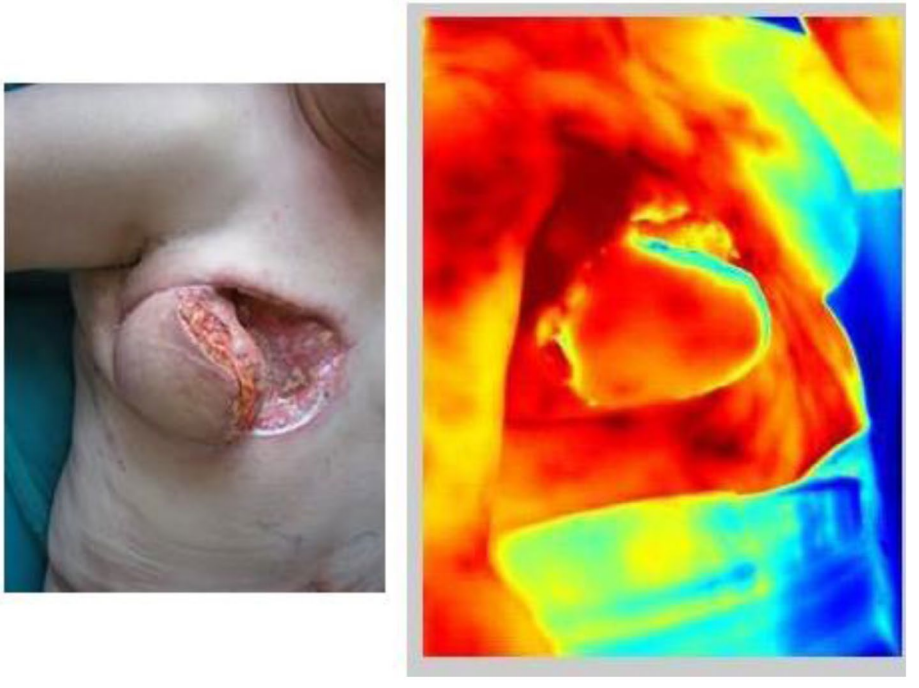

Figure 13. TRAM flap after debridement. Day 21 after surgical procedure.

The ADT based flap perfusion imaging method proved to be an effective tool for supporting surgeons decisions in the TRAM flap breast reconstruction. The dT_{norm} and t_{90_10n} parametric images are capable of detecting the exact location of perforators which supply the flap in blood and therefore their rejection would highly increase the risk of complications and flap necrosis. As it was shown the perfusion zones guidelines can be unreliable which can lead to complications.

One of its big advantages is the fact that it can be performed online in the operating room providing instantaneous feedback for the team of surgeons. The imaging procedure is less computational time consuming than the standard exponential parameterization methods. For the same sequence of 320 thermograms of the resolution 320×240 pix^2 processed at the same PC the time of new parameters computation took 0.1 s while the two-exponential optimisation took 10 min.

Summing up, the dT_{norm} and t_{90_10n} parametrization method thanks to its properties: non-invasiveness, reliability in the case of non-uniform excitation, thermal activity sensitivity as well as the ability to map perforators is good method for skin flap perfusion mapping. These features were confirmed via computer simulation and in the clinical research. The method can be also applied in solving other diagnostic/ imaging problems as for example post reconstruction reperfusion monitoring, surgical wound healing [13] or breast cancer detection [14].

Disclosure statement

No potential conflict of interest was reported by the authors.

Funding

This work has been partially supported by Statutory Funds of Electronics, Telecommunications and Informatics Faculty, Gdansk University of Technology.

References

[1] Thorne CH. Grabb and Smith plastic surgery. 7th ed., Chapter 61. Lippincott Williams & Wilkins; 2014. p. 643.
[2] Hartrampf Jr CR, Scheflan M, Black PW. Breast reconstruction with a transverse abdominal island flap. Plast Reconstr Surg. 1982;69:216–224.
[3] Creech B, Miller S. Evaluation of circulation in skin flaps. Skin flaps. Boston, MA: Little Brown; 1975.
[4] Yamaguchi S, De Lorenzi F, Petit JY, et al. The, "Perfusion Map" of the unipedicled TRAM flap to reduce postoperative partial necrosis. Ann Plast Surg. 2004;53:205–209.
[5] Miland ÅO., de Weerd L, Weum S, et al. Visualising skin perfusion in isolated human abdominal skin flaps using dynamic infrared thermography and indocyanine green fluorescence video angiography. Eur J Plast Surg. 2008;31(5):235–242.
[6] Nowakowski A. Quantitative active dynamic thermal IR–imaging and thermal tomography in medical diagnostics. In: Bronzino JB, editor. The biomedical engineering handbook. 3rd ed. Medical Devices and Systems. Boca Raton, FL: CRC Press; 2006. p. 22-1–22-30.
[7] Weerd L, Weum S, Mercer JB. Dynamic infrared thermography a useful tool in the preoperative planning of deep inferior epigastric perforator flaps. Ann Plast Surg. 2012 June;68(6):639–640; author reply 641.
[8] Weerd L, Weum S, Mercer JB. Detection of perforators using thermal imaging. Plast Reconstr Surg. 2014 Nov;134(5):850e–851e.
[9] Weum S, Mercer JB, Weerd L. Evaluation of dynamic infrared thermography as an alternative to CT angiography for perforator mapping in breast reconstruction: a clinical study Weum et al. BMC Med Imaging. 2016;16(1):43.
[10] Pennes HH. Analysis of tissue and arterial blood temperature in the resting forearm. J Appl Physiol. 1948;1:93–122.
[11] Khouri RK, Shaw WW. Monitoring of free flaps with surface-temperature recordings. Plast Reconstr Surg. 1992;89:495–499.
[12] Jones BM. Monitors for the cutaneous microcirculation. Plast Reconstr Surg. 1984;73:843–850.
[13] Nowakowski A, Siondalski P, Moderhak M, et al. A new diagnostic method for evaluation of cardiosurgery wound healing. Quant InfraRed Thermogr J 2016;13(1):19–34.
[14] Moderhak M. Analiza algorytmów diagnostyki termicznej w mammografii [PhD]. Gdansk Univerisity of Technology; 2013.
[15] Rumiski J, Kaczmarek M, Renkielska A, et al. Thermal parametric imaging in the evaluation of skin burn depth. IEEE Trans Biomed Eng. 2007;54(2):303–312.
[16] Renkielska A, Nowakowski A, Kaczmarek M, et al. Burn depths evaluation based on active dynamic IR thermal imaging – a preliminary study. Burns 2006;32:867–875.
[17] Renkielska A, Nowakowski A, Kaczmarek M, et al. Static thermography revisited – an adjunct method for determining the depth of the burn injury. Burns 2005;31(6):768–775.
[18] Merla A. Biomedical applications of functional infrared imaging. 21st Anuual Meeting of Houston Society of Engineering in Medicine and Biology; 2004; Houston TX, p. 690–693.
[19] Merla A, Di Donato L, Romani GL. Time recovery image: a diagnostic image technique based on the dynamic digital telethermography. Thermol Int. 2000;10:142.

[20] [Cited 2015 Dec 12]. Available from: http://www.orionairsales.co.uk/portable-air-conditioner-titan-cool-tc21-61-kw–21000-btu-industrial-unit-786p.asp
[21] Moderhak M. FFT spectra based matching algorithm for active dynamic thermography. Quant InfraRed Thermogr J. 2011;8(2):239–242.
[22] [Cited 2015 Dec 12]. Available from: www.sonomed.com.pl/veno.html